Applied Mathematics & Information Sciences
An International Journal

http://dx.doi.org/10.18576/amis/120118

On a Moving Four-Level λ-Type Atom Interacting with a Single-Mode Quantized Field in Intensity-Dependent Coupling

Tarek M. El-Shahat[1,*] *and Lamia E. Thabet*[2]

[1] Department of Mathematics, Faculty of Science, Al-Azhar University, 71524, Assiut, Egypt
[2] Department of Mathematics, Faculty of Science, Taiz University, Taiz, Yemen

Received: 15 Jul. 2017, Revised: 20 Sep. 2017, Accepted: 20 Oct. 2017
Published online: 1 Jan. 2018

Abstract: The interaction between a moving four-level atom and a single-mode cavity field are discussed in the presence of intensity dependent atom field coupling. For this purpose, we first demonstrate the feasibility of the effective Hamiltonian and evaluate the explicit time-dependent form of the state vector of the whole system by choosing special initial conditions for atom, field. Considering the field to be initially in a coherent state, and the atom is initially prepared in the excited state. The wave function is obtained in three different cases: resonance case, off-resonance case, finally we obtained it in the general form. We study the nonclassical features of the system such as Atomic inversion, Filed entropy, purity, Fidelity, Mandel Q-parameter, Mean photon number and normal squeezing. The results show that, The temporal evolution of field entropy (entanglement), Mandel parameter, mean photon number and normal squeezing are sensitive to intensity-dependent coupling, which changes the quantum statistical behaviour of the atom-field state to a full sub-Poissonian statistics. Finally, conclusions and some features and comments are given.

Keywords: Four-level atom, intensity-dependent coupling, purity, Fidelity, normal squeezing.

1 Introduction

Interaction of a two-level atom with a radiation field is the simplest problem in matter-radiation coupling. A model for the interaction, introduced by Jaynes and Cummings [1]. This model was generalized to describe The interaction model between a four-level atom and a single quantized mode of a radiation field, when the rotating wave approximation (RWA) considered [2,3,4,5,6]. There exists a theoretical motivation to include atomic motion effect to JCM, [7,8,9] have treated the JCM in the presence of atomic motion, by the use of analytic and numerical calculations.

On the other hand, we find that the most important problems in quantum optics are the studies of different systems interaction such as field-atom, atom-atom and the field-field [13,10]. One of the main consequences of the above interactions is the appearance of the entanglement [11,12]. Entanglement is a major supplier that distinguishes a key distinguishing element of quantum information theory from the classical one. Quantum entangled states, as a fundamental physical resource of quantum computation and quantum communication [14], quantum information processing [15,16,17], quantum cryptography [18,19]. There is a lot of attention we may focus on information entropies as a measure of entanglement in quantum information such as von Neumann entropy. The time evolution of the field entropy shows the degree of entanglement measurement;

In fact, Dynamics of a four-level atom interacting with a single mode of the radiation field in a lossless cavity has been discussed in detail from various points of view [20,21,22], and it has been generalized or extended further to incorporate the effects of the atomic motion and the field mode structure [23,24].
Schlicher and Joshi [23] have investigated the influences of the atomic motion and the field-mode structure on the atomic dynamics. To get a new insight into the relation between quantum entanglement of the atom-field system and nonclassicality of the light field, it is useful to investigate the atom-field entanglement under the nonclassical environment.

* Corresponding author e-mail: el_shahat@yahoo.com

We aim at extending the previously cited treatments to study the problem of a four-level atom in the consider configuration interacting with a single-mode field, in the presence of the intensity-dependent coupling, to investigate the properties of the degree of entanglement of the above mentioned systems from the view point of the Phoenix-Knight [25,27,26]. In this paper, while we refer to our earlier work [28], we have been studied the interaction between a four-level atom in our consideration model with a single mode field under multi-photon process with additional forms of nonlinearities of both field and atom-field coupling. has been studied in . Here, we study a moving atomic system of a four-level atom coupled to one mode electromagnetic cavity field in the presence of the intensity-dependent coupling,. We describe the Hamiltonian and derive the constants of motion. Also, this generalization takes into account the multi-photon processes. We derive the general form of the probability amplitudes for the considered system. Consequently, in this paper, after we have the exact analytical solution of the entire state vector of the system, We will experience the effects of the intensity-dependent coupling, on the time evolution of atomic inversion, field entropy, Q-Mandel parameter, mean photon number and normal squeezing. In this work, we observed that The temporal evolution of field entropy (entanglement), Mandel parameter, mean photon number and normal squeezing are susceptible to intensity-dependent coupling, which changes the quantum statistical behaviour of the atom-field state. Finally, we summarize our results.

2 Description of the model

In quantum mechanics, the most important step in studying any physical system is the construction of an appropriate Hamiltonian of the system. This goal is achieved by an exact view on the existing interactions between subsystems. Then, by solving the time-dependent Schrödinger equation, one may find the dynamical state of the system under study. Possible information arises from the wave function of the system.

The assumed model contains, in fact, three three-level subsystems with a common fourth level, one can distinguish here two subsystems in the ladder configuration (levels 1-4-3 and 2-4-3) and one subsystem in the lambda configuration (1-4-2) [28], (see Fig.1). Let us consider a model in which the single-mode electromagnetic field which oscillates with frequency Ω in an optical cavity interacts with a four-level λ-type atom an intensity-dependent coupling regime in an optical cavity field, when the coupling constants are equal. The atomic levels are indicated by $|1\rangle$, $|2\rangle$, $|3\rangle$ and $|4\rangle$ with energies $\omega_3 > \omega_4 > \omega_2 > \omega_1$, where the allowed transitions are $|3\rangle \longleftrightarrow |4\rangle$ and $|4\rangle \longleftrightarrow |1\rangle(|2\rangle)$. and the transition $|2\rangle \longleftrightarrow |1\rangle$ is forbidden (this assumption means that the atomic states $|1\rangle$ and $|2\rangle$ have the same number of photons).

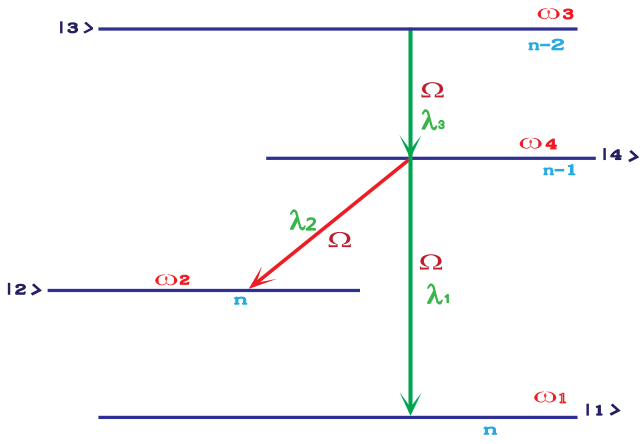

Fig. 1: The scheme for the considered atomic system

Also, we assume that the atom moves in the cavity and the atom-field interaction depends on the intensity of light. Based on the JCM formalism, as the full quantum mechanical approach to the problem, our proposed model can be appropriately described by the Hamiltonian (with $\hbar = 1$)

$$\hat{H} = \sum_{j=1}^{4} \hat{S}_{jj} + \Omega \widehat{a}^{\dagger}\widehat{a} + \lambda f(z)[(\hat{\Re}\hat{S}_{41} + \hat{\Re}^{\dagger}\hat{S}_{14}) + (\hat{\Re}\hat{S}_{42} + \hat{\Re}^{\dagger}S_{24}) + (\hat{\Re}\hat{S}_{34} + \hat{\Re}^{\dagger}S_{43})], \quad (1)$$

where $\widehat{S}_{jj}$ are the population operators satisfying the following commutation relations:

$$[\hat{S}_{ab}, \hat{S}_{cd}] = \hat{S}_{ad}\delta_{bc} - \hat{S}_{cb}\delta_{da}, [\hat{a}, \hat{S}_{ab}] = [\hat{a}^{\dagger}, \hat{S}_{ab}] = 0. \quad (2)$$

where δ_{da} is the Kroneker symbol and $\widehat{S}_{ab}|b\rangle = |a\rangle$. Else, $\hat{a}$, $\hat{a}^{\dagger}$ are respectively the bosonic annihilation and creation operators of the cavity field which satisfying the canonical commutation relation $[\hat{a}, \hat{a}^{\dagger}] = 1$ while $[\hat{a}, \hat{a}] = [\hat{a}^{\dagger}, \hat{a}^{\dagger}] = 0$, λ is the atom-field coupling constant, and ω_1, ω_2, ω_3 and ω_4 are the atomic energies of the level $|1\rangle$, $|2\rangle$, $|3\rangle$ and $|4\rangle$, respectively. Also, the deformed operators $\hat{\Re}$ and $\hat{\Re}^{\dagger}$ have been defined as:

$$\hat{\Re} = \hat{a}g(\hat{n}) = g(\hat{n}+1)\hat{a}, \hat{\Re}^{\dagger} = g(\hat{n})\hat{a}^{\dagger} = \hat{a}^{\dagger}g(\hat{n}+1). \quad (3)$$

with $\hat{n} = \hat{a}^{\dagger}\hat{a}$ as the number operator of the harmonic oscillator. Using the well-known Weyl-Heisenberg Lie algebra corresponding to the operators $\hat{a}$, $\hat{a}^{\dagger}$, $\hat{n}$ and the unity operator $\hat{I}$, plus the fact that the operator $\hat{n}$ commutes with the arbitrary function of itself, $g(\hat{n})$, the following communication relations clearly hold:

$$[\hat{\Re}, \hat{\Re}^{\dagger}] = (\hat{n}+1)g^2(\hat{n}+1) - \hat{n}g^2(\hat{n}),$$
$$[\hat{\Re}, \hat{n}] = \hat{\Re}, \qquad [\hat{\Re}^{\dagger}, \hat{n}] = -\hat{\Re}^{\dagger}. \quad (4)$$

where $g(\hat{n})$ is considered to be a Hermitian operator-valued function responsible for the intensity-dependent atom-field coupling. The influence of atomic motion in the model has been entered by the shape function $f(z)$. In view of the successful microwave-type-cavity-QED experiments as discussed above, we restrict the atomic motion along the cylindrical axis (e.g. the z-axis) of the cavity m so that only the z dependence of the cavity mode function needs to be considered. The atomic motion would be incorporated as [29]

$$f(z) \longmapsto f(vt) = p_1 + \sin(\frac{p_2 \pi v t}{L}), \tag{5}$$

where v denotes the atomic motion velocity, p_1 and p_2 are the atomic motion parameters well, if we put $p_1 = 2$ and $p_2 = 0$, then the shape function takes the form

$$\varpi(t) = \int_0^t (f(v\acute{t}))d\acute{t} = 2t, \tag{6}$$

which means, there is no atomic motion inside the cavity, but if $p_1 = 0$ and $p_2 = p$, where p represents the number of half-wave lengths of the field mode inside a cavity of length L, the shape function for a particular choice of the atomic motion velocity $v = \frac{gL}{\pi}$ will be

$$\varpi(t) = \int_0^t (f(v\acute{t}))d\acute{t} = \frac{1}{p\lambda}[1 - \cos(p\lambda t)]. \tag{7}$$

In order to obtain the state vector of the system, it should be suitable to rewrite the Hamiltonian (1) in the interaction picture,

$$\hat{H}_{IN} = e^{i\hat{H}_0 t}\widehat{H}_I e^{-i\hat{H}_0 t}, \tag{8}$$

which results in

$$\hat{H}_{IN} = \lambda f(z)\{\hat{a}(e^{-i(\Delta_1 t)}\hat{S}_{41} + e^{-i(\Delta_2 t)}\hat{S}_{42} + e^{-i(\Delta_3 t)}\hat{S}_{34}) + h.c\}, \tag{9}$$

where Δ_1, Δ_2, and Δ_3 are the detuning parameters and have been defined as

$$\begin{aligned} \Delta_1 &= \omega_1 - \omega_4 + \Omega, \\ \Delta_2 &= \omega_2 - \omega_4 + \Omega, \\ \Delta_3 &= \omega_4 - \omega_3 + \Omega. \end{aligned} \tag{10}$$

In what follows, we mind to derive the wave function of the model under consideration by using the time-dependent Schrödinger equation.

3 The wave function of the model and its solution

To obtain the explicit form of the wave function of the whole system, we solve the time-dependent Schrödinger equation

$$i\frac{\partial}{\partial t}|\Psi(t)\rangle = \hat{H}_{IN}|\Psi(t)\rangle. \tag{11}$$

For the assumed system, the wave function at any time t can be written in the following form:

$$|\Psi(t)\rangle = \sum_n q_n\Big[\Big(\psi_1(n,t)|1\rangle + \psi_2(n,t)|2\rangle\Big)\otimes|n\rangle + \psi_3(n-2,t)|3,n-2\rangle + \psi_4(n-1,t)|4,n-1\rangle\Big], \tag{12}$$

where q_n is the number-state expansion coefficients $q_n = \langle n|\Psi_F(t=0)\rangle$, for coherent state

$$q_n = e^{-\frac{|\alpha|^2}{2}}\frac{\alpha^n}{\sqrt{n!}}, \tag{13}$$

where $|\alpha|^2$ is the mean photon number in the initial state, $\alpha = |\alpha|\exp(i\eta)$, where η is the initial phase angle of the coherent field. Also, $\psi_1(n,t)$, $\psi_2(n,t)$, $\psi_3(n-2,t)$ and $\psi_4(n-1,t)$ are the atomic probability amplitudes which have to be determined.

The equations of motion for the probability amplitudes are obtained by substituting $|\Psi(t)\rangle$ from (12) and $\hat{H}_{IN}$ from (9) in the time-dependent Schrödinger equation (11). Consequently, one arrives at the following four first-order coupled differential equations:

$$i\frac{d}{dt}\begin{pmatrix}\psi_1(t)\\ \psi_2(t)\\ \psi_3(t)\\ \psi_4(t)\end{pmatrix} = \begin{pmatrix}0 & 0 & 0 & f_1 e^{i\delta_1}\\ 0 & 0 & 0 & f_1 e^{i\delta_2}\\ 0 & 0 & 0 & f_2 e^{-i\delta_3}\\ f_1 e^{-i\delta_1} & f_1 e^{-i\delta_2} & f_2 e^{i\delta_3} & 0\end{pmatrix}\begin{pmatrix}\psi_1(t)\\ \psi_2(t)\\ \psi_3(t)\\ \psi_4(t)\end{pmatrix} \tag{14}$$

where

$$\begin{aligned} &\delta_s = \Delta_s t, \qquad (s = 1,2,3), \\ &f_1 = \lambda\sqrt{n}g(\hat{n})f(z),\ f_2 = \lambda\sqrt{n-1}g(\hat{n}-1)f(z). \end{aligned} \tag{15}$$

We started by investigation the solution of the system (14). Let us suppose an atom takes place in the interaction to be prepared in a coherent superposition of its ground $|1\rangle$ and intermediate $|4\rangle$ states [30]. Thus, the initial state $|\Psi_{AF}(t=0)\rangle$ of the combined atom-field system may be written as

$$|\Psi_{AF}(t=0)\rangle = |\Psi_A(t=0)\rangle\otimes|\Psi_F(t=0)\rangle. \tag{16}$$

where $|\Psi_A(t=0)\rangle$, the initial state of the atom and $|\Psi_F(t=0)\rangle$, is the initial state of the field. So, the initial state is given by

$$|\Psi_{AF}(t=0)\rangle = \sum_{n=0}^{\infty} q_n[(\cos(\theta)|1,n\rangle + \sin(\theta)e^{i\phi}|4,n+1\rangle)], \tag{17}$$

where $\theta \in [0,\pi]$ denotes the coherence of the two level and $\phi \in [0,2\pi]$ is the relative phase between the upper and lower states of a two-level atom. It is clear that when the atom is initially prepared in its ground (intermediate) state $|1\rangle$ ($|4\rangle$), the value of the angle θ equal 0 and $(\pi/2)$. Now, we will resolve the above system in the three different cases as follow.

4 The solution in the resonance case

In this case, we assume that the cavity eigenfrequency is on resonance with the atomic transition frequency i.e., ($\Delta_s = 0$). Under the initial condition (17), the previous system (14) can be written as:

$$i\frac{d}{dt}\begin{pmatrix}\psi_1(t)\\ \psi_2(t)\\ \psi_3(t)\\ \psi_4(t)\end{pmatrix}=\begin{pmatrix}0&0&0&f_1\\ 0&0&0&f_1\\ 0&0&0&f_2\\ f_1&f_1&f_2&0\end{pmatrix}\begin{pmatrix}\psi_1(t)\\ \psi_2(t)\\ \psi_3(t)\\ \psi_4(t)\end{pmatrix} \tag{18}$$

After some lengthy but simple manipulations, the probability amplitudes $\psi_j(t)$ (specifying the explicit form of the state vector of whole system) may be found in the form

$$\begin{aligned}&\psi_1(n,t)=\wp_1+\wp_2\cos(Ft)+\wp_3\sin(Ft),\\ &\psi_2(n,t)=o_1+o_2\cos(Ft)+o_3\sin(Ft),\\ &\psi_3(n-2,t)=\varsigma_1+\varsigma_2\cos(Ft)+\varsigma_3\sin(Ft),\\ &\psi_4(n-1,t)=\aleph_1\cos(Ft)+\aleph_2\sin(Ft),\end{aligned} \tag{19}$$

where

$$\begin{aligned}F &= \sqrt{2f_1^2+f_2^2}.\\ \wp_1 &= \frac{1}{F^2}(f_1^2+f_2^2)\cos(\theta)),\\ \wp_2 &= \cos(\theta)-\frac{1}{F^2}(f_1^2+f_2^2)\cos(\theta),\\ \wp_3 &= (\frac{-i}{F})f_1\exp(-i\phi)\sin(\theta),\\ o_1 &= \frac{-1}{F^2}(f_1^2\cos(\theta)),\qquad o_2=-o_1,\\ o_3 &= \wp_3,\\ \varsigma_1 &= \frac{-1}{F^2}(f_1f_2\cos(\theta)),\qquad \varsigma_2=-\varsigma_1,\\ \varsigma_3 &= =(\frac{-i}{F})f_2\sin(\theta)\exp(-i\phi),\\ \aleph_1 &= \sin(\theta)\exp(-i\phi),\\ \aleph_2 &= (\frac{-i}{F})f_1\cos(\theta).\end{aligned} \tag{20}$$

5 The solution in the off-resonance case

In this case, we assume that the cavity eigenfrequency is off-resonance with the atomic transition frequency i.e., ($\Delta_s = \Delta$). To obtain an analytical solution for the coupled ordinary differential equations (14), we will use the same previous technique in the on resonant case, and after minor algebra, one can obtain the probability amplitudes $\psi_j(t)$ in the following form

$$\begin{aligned}\psi_1(n,t) &= \frac{-i(\frac{\Delta}{2})^3\gamma_1+(\frac{\Delta}{2})^2\gamma_2+(\frac{i\Delta}{2})\gamma_3-\gamma_4}{(x_1+\frac{i\Delta}{2})(x_2+\frac{i\Delta}{2})(x_3+\frac{i\Delta}{2})}\\ &+\{\frac{x_1^3\gamma_1+x_1^2\gamma_2+x_1\gamma_3+\gamma_4}{(x_1+\frac{i\Delta}{2})(x_1-x_2)(x_1-x_3)}\}\exp(x_1+\frac{i\Delta}{2})t\\ &+\{\frac{x_2^3\gamma_1+x_2^2\gamma_2+x_2\gamma_3+\gamma_4}{(x_2+\frac{i\Delta}{2})(x_2-x_1)(x_2-x_3)}\}\exp(x_2+\frac{i\Delta}{2})t\\ &+\{\frac{x_3^3\gamma_1+x_3^2\gamma_2+x_3\gamma_3+\gamma_4}{(x_3+\frac{i\Delta}{2})(x_3-x_1)(x_3-x_2)}\}\exp(x_3+\frac{i\Delta}{2})t\end{aligned} \tag{21}$$

$$\begin{aligned}\psi_2(n,t) &= \{\frac{(\frac{-i\Delta}{2})^2\alpha_1+(\frac{-i\Delta}{2})^2\alpha_2+\alpha_3}{(-x_1-\frac{i\Delta}{2})(-x_2-\frac{i\Delta}{2})(-x_3-\frac{i\Delta}{2})}\\ &+\{\frac{x_1^2\alpha_1+x_1\alpha_2+\alpha_3}{(x_1+\frac{i\Delta}{2})(x_1-x_2)(x_1-x_3)}\}\exp(x_1+\frac{i\Delta}{2})t\\ &+\{\frac{x_2^2\alpha_1+x_2\alpha_2+\alpha_3}{(x_2+\frac{i\Delta}{2})(x_2-x_1)(x_2-x_3)}\}\exp(x_2+\frac{i\Delta}{2})t\\ &+\{\frac{x_3^2\alpha_1+x_3\alpha_2+\alpha_3}{(x_3+\frac{i\Delta}{2})(x_3-x_1)(x_3-x_2)}\}\exp(x_3+\frac{i\Delta}{2})t,\end{aligned} \tag{22}$$

$$\begin{aligned}\psi_3(n-2,t) &= \{\frac{(\frac{-i\Delta}{2})^2\beta_1+(\frac{-i\Delta}{2})^2\beta_2+\beta_3}{(-x_1-\frac{i\Delta}{2})(-x_2-\frac{i\Delta}{2})(-x_3-\frac{i\Delta}{2})}\\ &+\{\frac{x_1^2\beta_1+x_1\beta_2+\beta_3}{(x_1+\frac{i\Delta}{2})(x_1-x_2)(x_1-x_3)}\}\exp(x_1-\frac{3i\Delta}{2})t\\ &+\{\frac{x_2^2\beta_1+x_2\beta_2+\beta_3}{(x_2+\frac{i\Delta}{2})(x_2-x_1)(x_2-x_3)}\}\exp(x_2-\frac{3i\Delta}{2})t\\ &+\{\frac{x_3^2\beta_1+x_3\beta_2+\beta_3}{(x_3+\frac{i\Delta}{2})(x_3-x_1)(x_3-x_2)}\}\exp(x_3-\frac{3i\Delta}{2})t\end{aligned} \tag{23}$$

$$\begin{aligned}\psi_4(n-1,t) &= \{\frac{(\frac{-i\Delta}{2})^3\xi_1+(\frac{-i\Delta}{2})^2\xi_2+(\frac{-i\Delta}{2})\xi_3+\xi_4}{(-x_1-\frac{i\Delta}{2})(-x_2-\frac{i\Delta}{2})(-x_3-\frac{i\Delta}{2})}\}\\ &\qquad\exp(-i\Delta t)\\ &+\{\frac{x_1^3\xi_1+x_1^2\xi_2+x_1\xi_3+\xi_4}{(x_1+\frac{i\Delta}{2})(x_1-x_2)(x_1-x_3)}\}\exp(x_1-\frac{i\Delta}{2})t\\ &+\{\frac{x_2^3\xi_1+x_2^2\xi_2+x_2\xi_3+\xi_4}{(x_2+\frac{i\Delta}{2})(x_2-x_1)(x_2-x_3)}\}\exp(x_2-\frac{i\Delta}{2})t\\ &+\{\frac{x_3^3\xi_1+x_3^2\xi_2+x_3\xi_3+\xi_4}{(x_3+\frac{i\Delta}{2})(x_3-x_1)(x_3-x_2)}\}\exp(x_3-\frac{i\Delta}{2})t\end{aligned} \tag{24}$$

with

$$x_\kappa = -\frac{1}{3}\delta_1 + \frac{2}{3}\sqrt{\delta_1^2 - 3\delta_2}\cos\left[\Theta + \frac{2}{3}(\kappa-1)\pi\right],$$
$$\kappa = 1,2,3.$$
$$\Theta = \frac{1}{3}\cos^{-1}\left[\frac{9\delta_1\delta_2 - 2\delta_1^3 - 27\delta_3}{2(\delta_1^2 - 3\delta_2)^{\frac{3}{2}}}\right]. \quad (25)$$

and

$$\delta_1 = -3(i\Delta/2), \delta_2 = (\frac{\Delta}{2})^2 + 2f_1^2 + f_2^2,$$
$$\delta_3 = i\left[\frac{\Delta}{2}f_2^2 - 3\Delta f_1^2 - 3(\frac{\Delta}{2})^3\right] \quad (26)$$

also

$$\gamma_1 = \cos(\theta),$$
$$\gamma_2 = -i\Big\{3(\Delta/2)\cos(\theta) + f_1\sin(\theta)e^{-i\phi}\Big\},$$
$$\gamma_3 = \Big(f_1^2 + f_2^2 + (\Delta/2)^2\Big)\cos(\theta) - \Delta f_1\sin(\theta)e^{-i\phi},$$
$$\gamma_4 = (i\Delta/2)\Big\{\Big(f_2^2 - 3f_1^2 - 3(\Delta/2)^2\Big)\cos(\theta)$$
$$-3(\Delta/2)f_1\sin(\theta)e^{-i\phi}\Big\},$$
$$\alpha_1 = -if_1\sin(\theta)e^{-i\phi},$$
$$\alpha_2 = -f_1^2\cos(\theta) - \Delta f_1\sin(\theta)e^{-i\phi},$$
$$\alpha_3 = 3i(\Delta/2)\Big\{f_1^2\cos(\theta) - (\Delta/2)f_1\sin(\theta)e^{-i\phi}\Big\},$$
$$\beta_1 = -if_2\sin(\theta)e^{-i\phi},$$
$$\beta_2 = \Delta f_2\sin(\theta/2)e^{-i\phi} - f_1f_2\cos(\theta/2),$$
$$\beta_3 = i(\Delta/2)\Big\{\Delta/2\sin(\theta)e^{-i\phi} - f_1\cos(\theta)\Big\}f_2,$$
$$\xi_1 = \sin(\theta)e^{-i\phi},$$
$$\xi_2 = -if_1\cos(\theta) - (i\Delta/2)\sin(\theta)e^{-i\phi},$$
$$\xi_3 = (5/4)\Delta^2\sin(\theta)e^{-i\phi} - \Delta f_1\cos(\theta),$$
$$\xi_4 = 3i(\Delta/2)^3\sin(\theta)e^{-i\phi} - 3if_1(\Delta/2)^2\cos(\theta) \quad (27)$$

6 The general solution

On the other hand, in the non-resonance case ($\Delta_r \neq \Delta$), By assuming $\psi_3(t) = e^{i\mu_j t}$ the coupled ordinary differential equations (14), lead us to the fourth-order algebraic equation:

$$\mu^4 + \varrho_3\mu^3 + \varrho_2\mu^2 + \varrho_1\mu + a_0 = 0. \quad (28)$$

where

$$\varrho_3 = y_1 + \Delta_3 + \Delta_2, \qquad \varrho_2 = y_2 + y_1(\Delta_2 + \Delta_3), \quad (29)$$
$$\varrho_1 = y_3 + (\Delta_3 + \Delta_2)y_2 - \epsilon f_1^2, \qquad \varrho_0 = y_3(\Delta_2 + \Delta_3). \quad (30)$$

The four roots of the quartic equation (28) are given by using MATHEMATICA in the following form [54]:

$$\mu_{1(2)} = -\frac{\varrho_3}{4} - \frac{1}{2}\sqrt{(u_1/3v_2) + (v_2/3) + u_2} \mp \frac{1}{2}(\sqrt{w_2 - (w_3/4w_1)},$$
$$\mu_{3(4)} = -\frac{\varrho_3}{4} + \frac{1}{2}\sqrt{(u_1/3v_2) + (v_2/3) + u_2} \mp \frac{1}{2}(\sqrt{w_2 + (w_3/4w_1)}, \quad (31)$$

where

$$w_1 = \sqrt{u_1 + (u_1/3v_2) + (v_2/3)},$$
$$w_2 = 2u_2 - (u_1/3v_2) - (v_2/3),$$
$$w_3 = -8\varrho_1 + 4\varrho_2\varrho_3 - \varrho_3^3.$$
$$u_1 = 12\varrho_0 + \varrho_2^2 - 3\varrho_1\varrho_3,$$
$$u_2 = (-2\varrho_2/3) + (\varrho_3^2/4), \quad (32)$$
$$v_1 = 27\varrho_1^2 - 72\varrho_0\varrho_2 + 2\varrho_2^3 - 9\varrho_1\varrho_2\varrho_3 + 27\varrho_0\varrho_3^2,$$
$$v_2 = \left[\left(v_1 + \sqrt{-4u_1^3 + v_1^2}\right)/2\right]^{\frac{1}{3}}.$$

By considering $\psi_3(t)$ as a linear combination of $e^{i\mu_{\mathcal{J}}t}$ and after straightforward calculations, we obtain the probability amplitudes in the form

$$\psi_1(t) = \frac{-1}{\epsilon f_1 f_2}\sum_j^4 C_j(\mu_j^3 + z_1\mu_j^2 + z_2\mu_j + z_3)e^{i(\mu_j+\Delta_3+\Delta_1)t},$$
$$\psi_2(t) = \frac{1}{\epsilon f_1 f_2}\sum_j^4 C_j(\mu_j^3 + y_1\mu_j^2 + y_2\mu_j + y_3)e^{i(\mu_j+\Delta_3+\Delta_2)t},$$
$$\psi_3(t) = \sum_j^4 C_j e^{i\mu_j t},$$
$$\psi_4(t) = \frac{-1}{f_2}\sum_j^4 C_j\mu_j e^{i(\mu_j+\Delta_3)t}, \quad (33)$$

with

$$\epsilon = \Delta_1 - \Delta_2,$$
$$z_1 = 2\Delta_3 + \Delta_2,$$
$$z_2 = \Delta_3^2 - f_2^2 - 2f_1^2 + \Delta_2\Delta_3,$$
$$z_3 = -f_2^2(\Delta_2 + \Delta_3),$$
$$y_1 = 2\Delta_3 + \Delta_1,$$
$$y_2 = \Delta_3^2 - f_2^2 - 2f_1^2 + \Delta_1\Delta_3,$$
$$y_3 = -(\Delta_1 + \Delta_3)f_2^2. \quad (34)$$

where

$$C_j = \frac{\Im_1(\mu_\ell+\mu_k+\mu_m) + \Im_2(\mu_{\ell k}+\mu_{\ell m}+\mu_{km}) + \Im_3}{\mu_{j\ell}\mu_{jm}\mu_{jk}},$$
$$\mu_{jk} = \mu_j - \mu_k, j \neq k \neq \ell \neq m = 1,2,3,4. \quad (35)$$

with

$$\Im_1 = -\Big\{\Delta_3 f_2\sin(\theta)e^{-i\phi} + f_1 f_2\cos(\theta)\Big\},$$
$$\Im_2 = -f_2\sin(\theta)e^{-i\phi}, \quad (36)$$
$$\Im_3 = -\Big\{f_2(\Delta_3^2 + f_2^2 + 2f_1^2)\sin(\theta)e^{-i\phi} + y_1 f_1 f_2\cos(\theta)\Big\}.$$

Due to the apparent entanglement feature of the considered atoms-field system, it is natural to investigate the amount of this pure quantum quantity at first, the above calculations can be used to discuss some properties of the considered system. For achieving to this purpose, several measures of entanglement have been proposed such as field entropy, purity, Fidelity and so on, to discuss the degree of entanglement for the different parts of the considered system.

7 The Atomic inversion

We are now in a position to examine the atomic dynamics, in particular the dynamics of an important quantity, namely atomic inversion. The atomic inversion, which is introduced as the difference between the excited-state and ground-state probabilities, may be defined as follows [31,32]:

$$W(t) = \rho_{33} - \rho_{11}, \tag{37}$$

where

$$\rho_{ij} = \sum_{n=0}^{\infty} \langle n|i|\psi\rangle\langle\psi|n|j\rangle, \qquad i,j = 1,2,3,4. \tag{38}$$

In what follows, we shall study numerically the influence of the intensity dependent coupling on the dynamical behavior of the atomic inversion $W(t)$, given by Eq.37 are shown in Fig.2 for different atomic motion states and different field-mode structure parameter p. Fig.2a(left plots) displays the case when the atomic motion is not taken into account $p_1 = 2, p_2 = 0$, while Fig.2a(right plots) illustrate the cases when the atom is in motion at the velocity $V = \frac{gL}{\pi}$ for parameter $p_1 = 0, p_2 = 2$, $p_2 = 6$, respectively. The above figures show that the atomic motion leads to the periodic evolution and disappearance of the collapse of the atomic inversion. Fig.2b shown that the number of fluctuation are very high (increase of the number of oscillations and there is no collapse for the case of fixed motion, but when the atom is in motion the atomic inversion shows a regular oscillations). For the intensity dependent coupling $g(n) = \sqrt{n+\upsilon}$, Fig.2c shows clearly the collapse-revival phenomenon, the atomic inversion leads to increase of the periodicity. The base line of $W(t)$ is shifted downward which means more energy is stored in the field.

8 Mean photon number

For any operator $\hat{O}$ the expectation values are given by $\langle\Psi(t)|\hat{O}|\Psi(t)\rangle$. For instance, the mean photon number $\langle\hat{a}^{\dagger}(t)\hat{a}(t)\rangle$ can be written as

$$\langle\hat{a}^{\dagger}(t)\hat{a}(t)\rangle = \overline{n} - 2\sum_{n} P(n)|\psi_3(n-2,t)|^2 \tag{39}$$

$$-\sum_{n} P(n)|\psi_4(n-1,t)|^2, \tag{40}$$

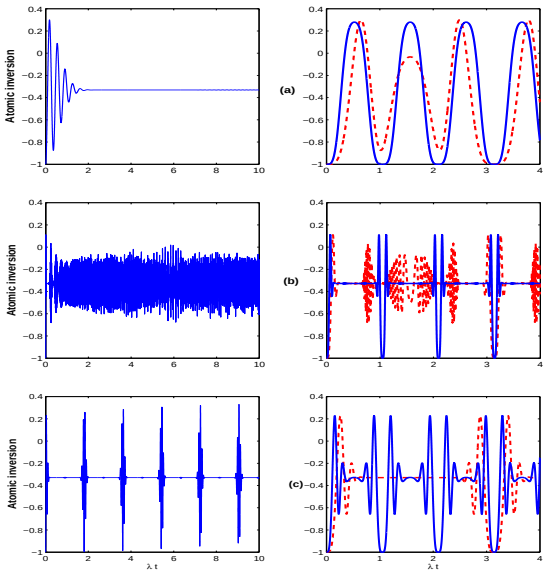

Fig. 2: Atomic inversion in terms of the scaled time, λt, (a) $g(n) = 1$, (b) $g(n) = n$, (c) $g(n) = \sqrt{n+\upsilon}, \upsilon = 3$, $\phi = \pi/7$, $\theta = 0$, when the atom and field are assumed to be initially in an superposition state and in a coherent state with $|\alpha|^2 = 25$ respectively. The left plots correspond to the influence of intensity dependent coupling for fixed p ($p = 2$) and the right plots show the effect of the atomic motion and field-mode structure by considering $p = 2$ (dashed line), and $p = 6$ (solid line).

where $P(n)$ is the distribution function for the coherent field. It is important to mention that the mean photon number is used to investigate the collapses revivals phenomenon. Now, we turn our attention to discuss the time evolution of the mean photon number which shows the collapses-revivals phenomenon.

Fig.3 shows the evolution of the mean photon number against a scaled time λt. The left plots of this figure show the influence of intensity time dependent by selecting the fixed value of the field-mode structure parameter $p_1 = 2$. Also, the effect of this parameter by considering different values of p in the shape function $f(z)$ is discussed in the right plots. We take the nonlinearity functions as $g(n) = 1$ (no intensity dependence, Fig.3(a)), $g(n) = n$ (Fig.3(b)) and $g(n) = \sqrt{n+\upsilon}$ (Fig.3(c)). An overview on the mean photon number distribution in an explicit manner [33,34]. The left plots of Figs.3(a,b,c), we can see the collapse-revival phenomena as a nonclassical sign in all frames of these figures except the right plots of Figs. 3(c)(left plot) which have a regular behavior in scaled time. The Fig.3(a)(left plot) shown that the collapse and revival occurs, and the oscillations decrease with $g(n) = 1$. We see that the mean photon evolves periodically and the oscillations increases whereas the amplitude decreases with increase in the scaled time. Also, the collapse and

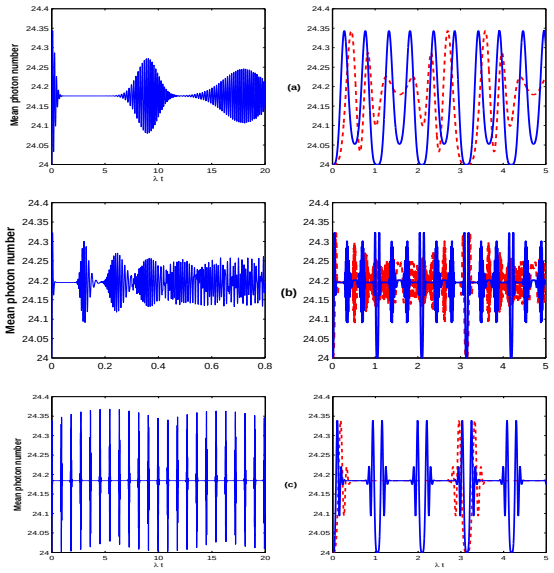

Fig. 3: Mean photon number in terms of the scaled time λt, $\bar{n} = 20$, $\phi = \pi/2$, $\theta = \pi/3$, for chosen parameters similar to Fig. 2.

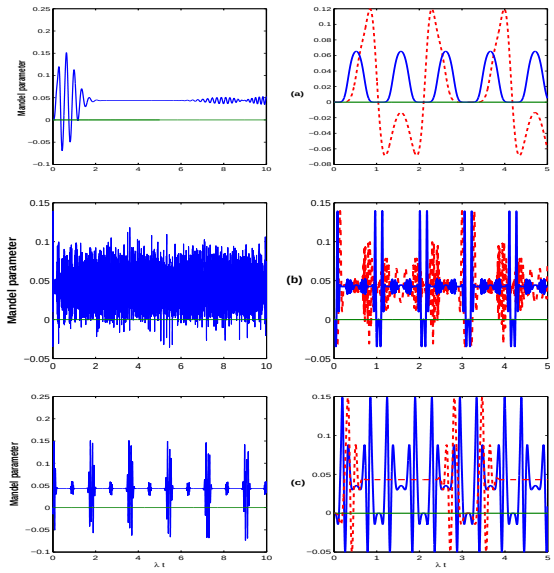

Fig. 4: The time evolution of the Mandel Q- parameter in terms of the scaled time λt, $\phi = \pi/2$, $\theta = \pi$, for chosen parameters similar to Fig 2.

revival phenomenon is very obvious, and the oscillations disappear very fast away in aa short time, see Figs.3(b)(left plot). The right plots of Figs.3(a,b,c), which have a regular behavior in scaled time. In general, comparing Figs.3(a) and Figs.3(c) indicates that intensity time dependent effect causes a decrease in the maximum values of mean number of photons (the same situation is observed in Figs.3(a) and 3(c)). In the nonlinear case, when the intensity time dependent are present, the collapse-revival phenomenon is clearly occurred, for $g(n) = \sqrt{n+\upsilon}$, $p = 2$, in the right plots of Figs.3(c) the collapses are longer and the overlap of the succeeding revivals is weaker, but for $p = 6$ the collapses are shorter and the overlap of the succeeding revivals is strong, see right frames of (b) and (c)in Fig.3.

9 Q-Mandel parameter

Q-Mandel parameter measures the departure of the occupation number distribution from Poissonian statistics. It was introduced in quantum optics by L. Mandel [35]. It is a convenient way to distinguish non-classical states with negative values to illustrate a sub-Poissonian statistics, which have no classical analog. It is defined as the normalized variance of the boson distribution:

$$Q(t) = \frac{\langle(\hat{a}^{\dagger}(t)\hat{a}(t))^2\rangle - \langle\hat{a}^{\dagger}(t)\hat{a}(t)\rangle^2}{\langle\hat{a}^{\dagger}(t)\hat{a}(t)\rangle} - 1, \tag{41}$$

where $\langle\hat{a}^{\dagger}(t)\hat{a}(t)\rangle$ is the photon number operator which given in (39), and

$$\langle(\hat{a}^{\dagger}\hat{a})^2\rangle = \bar{n}(\bar{n}+1) + 4\sum_n (n-1)P_n|\psi_3(n-2,t)|^2 + \sum_n (1-2n)P_n|\psi_4(n-1,t)|^2. \tag{42}$$

We examine the effects of the intensity dependent coupling on the temporal evolution of the Mandel Q-parameter in Figs.4 for single photon processes. The behavior can be seen in the left plots of Fig.4(a) for the fixed motion case with $g(n) = 1$, shows the super-Poissonian statistics of field as a long collapse at all times. But, from the right plots of Fig.4(a), where the intensity-dependent coupling is present, we observe that the Mandel parameter is always positive, the right plot of Fig.4(a), shows the full super-Poissonian statistics of field at all times (solid line).

The behavior can be seen in the right plots of Fig.4(b) for the motion case with $g(n) = n$. But, from the left plots of Fig.4(b), where the intensity-dependent coupling is present, we observe that the Mandel parameter is always Rabi-oscillations. Also, the right plot of Fig.4(b), which is plotted for $p_1 = 0$, $p_2 = 2,6$, shows that, the intensity-dependent coupling remove the sub-Poissonian statistics parts of the field.

For $g(n) = \sqrt{n+\upsilon}$, in the left plots of Fig.4(c), Mandel parameter varies between positive and negative values, which means that the photons display super-Poissonian or sub-Poissonian statistics for different intervals of times,

alternatively. Typical collapse-revival phenomenon is clearly seen for all the time in left plots of Fig.4(c). Moreover, the possess a periodic behaviour in right plots of Fig.4(c) leads to the observation of the collapse and revivals which are a nonclassical feature.

10 Field Entropy

The quantum dynamics described by the Hamiltonian (1) leads to an entanglement of the atomic system (field and atom). Quantum mechanically, the entropy is defined by:

$$S = -\mathbf{Tr}(\rho \ln \rho). \tag{43}$$

where ρ is the density operator for a given quantum

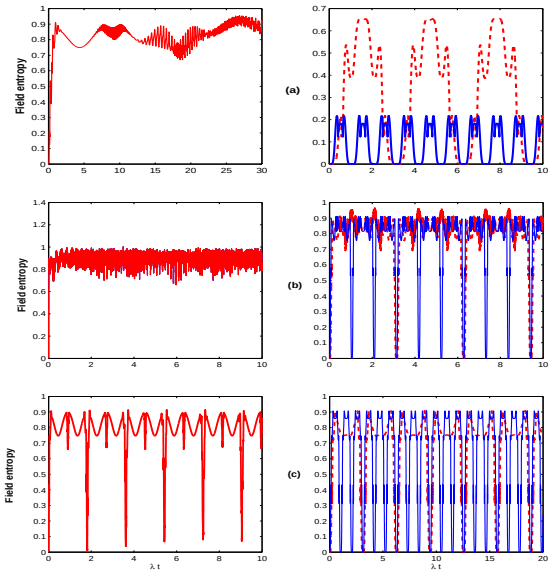

Fig. 5: The Field entropy in terms of the scaled time λt, $\bar{n} = 20$, $\phi = \pi/2$; $\theta = \pi/3$, for chosen parameters similar to Fig.2.

system with Boltzmann's constant is equal to 1. If S is the entropy of the composite system and $S_{A(F)}$ is the entropy of the atom (field), these the entropies satisfy the inequalities $|S_A - S_F| \leq S \leq |S_A + S_F|$ [36,37]. We calculate the atomic entropy S_A but calculation of the field entropy S_F is more Complicated. If the density operator ρ represents a pure state, then $S = 0$, and if it represents mixed state then $S \neq 0$. The entropies of the atom and the field, when analyzed as a separate system, are defined through the corresponding reduced density operator by

$$S_{A(F)} = -\mathbf{Tr}_{A(F)}(\rho_{A(F)} \ln \rho_{A(F)}). \tag{44}$$

The reduced density matrix of the atom required for evaluating (44) is given by:

$$\rho_A = \mathbf{Tr}_F |\Psi(t)\rangle\langle\Psi(t)| = \begin{pmatrix} \rho_{33} & \rho_{34} & \rho_{32} & \rho_{31} \\ \rho_{43} & \rho_{44} & \rho_{42} & \rho_{41} \\ \rho_{23} & \rho_{24} & \rho_{22} & \rho_{21} \\ \rho_{13} & \rho_{14} & \rho_{12} & \rho_{11} \end{pmatrix} \tag{45}$$

The matrix in Eq.(45) are given, for instance, by

$$\begin{aligned}
\rho_{11} &= \sum_{n=0}^{\infty} p_n |\psi_1(n,t)|^2, \\
\rho_{22} &= \sum_{n=0}^{\infty} p_n |\psi_2(n,t)|^2, \\
\rho_{33} &= \sum_{n=0}^{\infty} p_n |\psi_3(n-2,t)|^2, \\
\rho_{44} &= \sum_{n=0}^{\infty} p_n |\psi_4(n-1,t)|^2, \\
\rho_{12} &= \sum_{n=0}^{\infty} p_n \psi_1(n,t)\psi_2^*(n,t), \\
\rho_{13} &= \sum_{n=0}^{\infty} q_{n-2} q_n^* \psi_1(n-2,t)\psi_3^*(n-2,t), \\
\rho_{14} &= \sum_{n=0}^{\infty} q_{n-1} q_n^* \psi_1(n-1,t)\psi_4^*(n-1,t), \\
\rho_{23} &= \sum_{n=0}^{\infty} q_{n-2} q_n^* \psi_2(n-2,t)\psi_3^*(n-2,t), \\
\rho_{24} &= \sum_{n=0}^{\infty} q_{n-1} q_n^* \psi_2(n-1,t)\psi_4^*(n-1,t), \\
\rho_{34} &= \sum_{n=0}^{\infty} q_n q_{n-1}^* \psi_3(n-1,t)\psi_4^*(n-1,t),
\end{aligned} \tag{46}$$

where in all of the above relations, $P_n = |q_n|^2$ is the distribution of the initial radiation field, and ψ_1, ψ_2, ψ_3 and ψ_4 are the atomic probability amplitudes derived in (19). Since the trace is invariant under a similarity transformation, we can go to a basis in which the density matrix of the field is diagonal and we can express the field entropy $S_F(t)$ in terms of the eigenvalues $\gamma_F^{(j)}(t)$, $j = 1,2,3,4$ of the reduced density operator. For the considered atomic system the eigenvalues of the density matrix (45) are the four roots of the following equation:

$$\gamma^4 + \Re_0\gamma^3 + \Re_1\gamma^2 + \Re_2\gamma + \Re_3 = 0, \tag{47}$$

where

$$\begin{aligned}
\Re_0 &= -(\rho_{11}+\rho_{22}+\rho_{33}+\rho_{44}),\\
\Re_1 &= \sum_j [\rho_{jj}\rho_{kk}-|\rho_{jk}|^2], j<k,\\
\Re_2 &= \sum_{j\neq k\neq \ell}\rho_{jj}|\rho_{k\ell}|^2-\sum_{j<k<\ell}\rho_{jj}\rho_{kk}\rho_{\ell\ell}-[\rho_{12}\rho_{23}\rho_{31}\\
&\quad +\rho_{12}\rho_{24}\rho_{41}+\rho_{13}\rho_{34}\rho_{41}+\rho_{23}\rho_{34}\rho_{42}+h.c],\\
\Re_3 &= \rho_{11}\rho_{22}\rho_{33}\rho_{44}+\sum_{j\neq k<\ell<m}\rho_{jj}[\rho_{k\ell}\rho_{\ell m}\rho_{mk}+h.c]\\
&\quad +\sum_{j<k<\ell<m}|\rho_{jk}|^2|\rho_{\ell m}|^2\\
&\quad -\sum_{j<k\neq\ell\neq m}\rho_{jj}\rho_{kk}|\rho_{\ell m}|^2-[\rho_{12}\rho_{23}\rho_{34}\rho_{41}+\\
&\quad \rho_{12}\rho_{24}\rho_{43}\rho_{31}+\rho_{13}\rho_{34}\rho_{42}\rho_{21}+h.c].
\end{aligned} \tag{48}$$

It is worth to mention that the four roots of (47) are given as shown previously by using MATHEMATICA program.

Fig.5 shows the time evolution of the field entropy against the scaled time λt for the initial mean number of photons fixed at $\bar{n}=25$. These plots illustrate the influences of intensity-dependent coupling by considering some particular operator-valued functions and atomic motion together with field-mode structure by considering different values of p in the shape function $f(z)$. when the atomic motion is not taken into consideration, the evolution of the field entropy is not periodical (see Fig.5(a,b,c)(left plots). Fig.5(a,b,c)(right plots) describes the influences of the atomic motion and the field-mode structure on the dynamic properties of the field entropy. These figures illustrate that the atomic motion leads to the periodic evolution of the field entropy, and an increase in parameter p results in not only decreasing of the evolution period of field entropy but also shortening in the amplitude of the field entropy. All these characteristics can be returned to the change in the atom-field interaction time due to atomic motion. This is due to the difference of the field entropy parameters between the two cases in which the atomic motion is neglected and taken into account results from the time factor. The time factor is the scaled time λt when the atomic motion is neglected, and is $\varpi(t)$ when the atomic motion is Taken into consideration, we have $\varpi(t)=\frac{1}{p}[1-\cos(p\lambda t)]$. It is observed that $\lambda\varpi(t)$ is a periodical function, this periodicity leads to the periodicities of evolution of the field entropy.

11 Purity

Entanglement is one of the most essential characteristics of the quantum mechanical systems which plays an important role within new information technologies. Also, It's important to resource in many interesting applications in fields related to quantum computation as well as quantum information [38] However, the appearance of entanglement in the interaction between field and matter in a cavity is of special interest, in which the atom field interaction produces the entangled state. The purity $P(t)$ of the system Can be used as a good a tool designed to give information about the entanglement of the components of the system. For this reason we devote the present section to discuss the purity of the system under consideration. The purity of the field state can be determined from the quantity [39,40]

$$P(t)=Tr(\rho^2(t)), \tag{49}$$

where ρ is the field-reduced density matrix. A necessary and sufficient condition for the ensemble to be described in terms of a pure state is that $Tr(\rho^2(t)=1$, in this case clearly a state-vector description of each individual system of the ensemble is possible. For the case $Tr(\rho^2(t)<1$, the field will be in a statistical mixture state. From Equation (45), it is easy to show that

$$\begin{aligned}
P(t) &= \rho_{11}^2+\rho_{22}^2+\rho_{33}^2+\rho_{44}^2+2|\rho_{12}|^2+2|\rho_{13}|^2\\
&\quad +2|\rho_{14}|^2+2|\rho_{23}|^2+2|\rho_{24}|^2+2|\rho_{34}|^2.
\end{aligned} \tag{50}$$

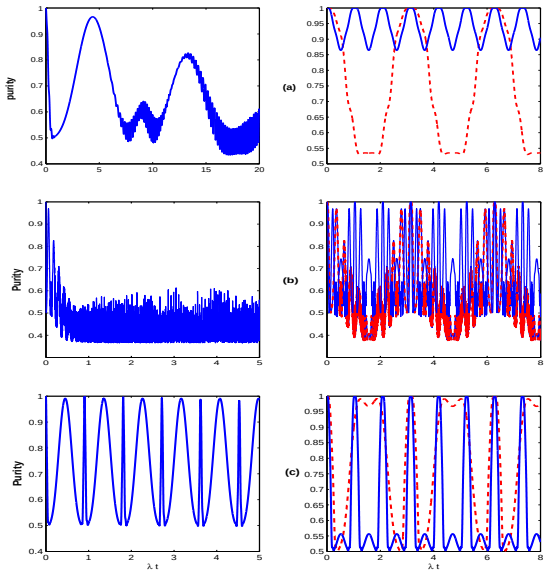

Fig. 6: The purity in terms of the scaled time λt, $\phi=\pi./4$, $\theta=\pi/4$, for chosen parameters similar to Fig 2.

From (50), the purity can range between zero, corresponding to a completely pure state, and $(1-\frac{1}{d})$, corresponding to a completely mixed state (here, d is the dimension of the density matrix). Based on the analytical solution in the previous section, we shall examine the evolution in time of the purity.

We have plotted the purity in Figs.6(a,b,c) against the scaled λt for both the atomic and field subsystems for some chosen parameters, in Fig.6a(left plot) corresponds to the fixed motion, shown that irregular oscillatory behavior for the time evolution of the purity, it is obvious that the purity of the system pulled down compared with the effect of $g(n)$ we set three different values of intensity coupling Fig.6a $g(n) = 1$, Fig.6b $g(n) = n$, Fig.6c $g(n) = \sqrt{n+\upsilon}$, with all other parameters, we notice that the purity becomes unstable and less than 0.5, So, the field is in statistically mixed state.

Fig.6(a,b,c)(right plots) displays the case when the atomic motion is taken into account $p_1 = 0, p_2 = 2$. The purity have regular and periodic oscillations when the $g(n) = 1$ see Fig.6a (right plot) the purity takes its maximum value (solid line), so we arrive to pure state, it is reach to disentanglement. But for $p_2 = 6$ (dashed line) the purity to go down to 0.5, we show that by an increase in P, the intervals of time will be shorter in which the entanglement between atom and field remains nearly at its minimum value.

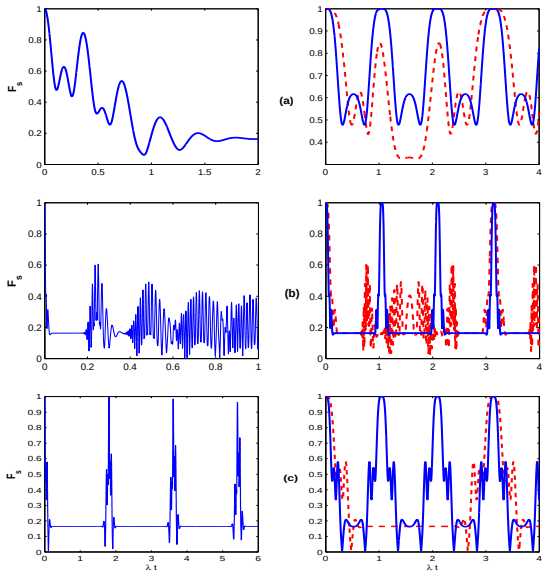

Fig. 7: The Fidelity in terms of the scaled time λt, $\bar{n} = 25$, $\phi = 0$; $\theta = \pi/3$, for chosen parameters similar to Fig 2.

12 Fidelity

The concept of the fidelity emerge from the mathematical representation for the purification of mixed states. Any mixed state can be represented as a subsystem of a pure state in a larger Hilbert space. The entanglement of a pure state may cause the states of subsystems to be mixed. The fidelity is usually used to measure how well the channel preserves the entanglement. In this section, we calculate the fidelity which plays the role of the transition between a pure state $|\Psi(0)\rangle$ and the state described by $\rho(t) = |\Psi\rangle\langle(t)\Psi(t)|$. This is equal to the square root of the overlap between the state $|\Psi(0)\rangle$ and the state defined by $\rho(t)$. The fidelity is given by the form [41, **?**],

$$F(t) = \sqrt{\langle\Psi(0)|\rho(t)|\Psi(0)\rangle} = |\langle\Psi(0)|\Psi(t)\rangle|, \tag{51}$$

The evolutions of the fidelities are plotted as functions of scaled time λt following. It can be seen from the figure that the time evolutions of fidelities are more complicated. Fig.1 presents fidelity for three different values of intensity dependent coupling $g(n)$. For $g(n) = 1$ the time evolutions of fidelity of quantum information obviously show the quantum collapse and revival in the system, and the fidelity decreases gradually. It means that the distortion increases gradually. With the $g(n) = n$, the evolution of the fidelities shows the irregular oscillations, and amplitude of them shows more or less decrease, implying that the quantum state fidelity is modulated by the initial field of number state. However, the nature that the evolutions of fidelity for $g(n) = \sqrt{n+\upsilon}$, exhibit oscillations with equiamplitude as is observed, the fidelity can become unity or approximately unity at some proper values of time. So, the fidelities are better than those for $g(n) = 1, n$ are conserved well. In comparison between Fig.a7(right plots) and Fig.7c(right plots), its can be seen from the figures the fidelities of quantum state of the system, the evolutions of fidelity give more regular oscillation, with equiamplitude and perfect periodicity and the amplitude equal to 1 for $g(n) = \sqrt{n+\upsilon}$.

13 Squeezing: normal and higher orders

In quantum optics, squeezing phenomenon is describes by decreasing the quantum fluctuations in one of the field quadratures with an increase in the corresponding conjugate quadrature. This parameter has been defined in various ways. As some examples, one may refer to first-order and higher-order squeezing. We define the following Hermitian operators:

$$\widehat{X}_k = \frac{1}{2}(\widehat{a}^k + \widehat{a}^{\dagger k}),$$
$$\widehat{y}_k = \frac{1}{2i}(\widehat{a}^k - \widehat{a}^{\dagger k}), k = 1, 2, 3, .. \tag{52}$$

where k indicates the order of squeezing of the radiation field. It is worth noticing that higher order squeezing may be generated in higher-order harmonics [43].

14 Normal (quadrature) squeezing

Setting $k = 1$ in (52), the X_1 and Y_1 quadratures obey the commutation relation $[X_1, Y_1] = i/2$. Consequently, the

uncertainty relation for such operators reads as $(\Delta X_1)^2$ $(\Delta Y_1)^2 \geq 1/16$, where $\langle \Delta Z_1)^2\rangle = \langle Z_1^2\rangle - \langle Z_1\rangle^2$ and $Z_1 = X_1$ or Y_1 and (ΔX_1) and (ΔY_1) are the uncertainties in the quadrature operators X_1 and Y_1, respectively. A state is squeezed in $X_1(Y_1)$ if $(\Delta X_1)^2 < 0.25$ or $((\Delta Y_1))^2 < 0.25$), or equivalently by defining

$$S_X^{(1)} = 4(\Delta X_1)^2 - 1, S_Y^{(1)} = 4(\Delta Y_1)^2 - 1, \tag{53}$$

squeezing occurs in $X_1(Y_1)$ component respectively if $1 < S_X^{(1)} < 0$ $(1 < S_Y^{(1)} < 0)$. So the parameters in (12) sometimes have been called the normalized squeezing parameters. These parameters can be rewritten as:

$$\begin{aligned} S_X^{(1)} &= \left[2\langle \hat{a}^\dagger \widehat{a}\rangle + \langle \hat{a}^2\rangle + \langle \hat{a}^{\dagger 2}\rangle - (\langle \hat{a}\rangle + \langle \hat{a}^\dagger\rangle)^2\right], \\ S_Y^{(1)} &= \left[2\langle \hat{a}^\dagger \hat{a}\rangle - \langle \hat{a}^2\rangle - \langle \hat{a}^{\dagger 2}\rangle + (\langle \hat{a}\rangle - \langle \hat{a}^\dagger\rangle)^2\right]. \end{aligned} \tag{54}$$

where $\langle \hat{a}^\dagger \hat{a}\rangle$ has been given by (39).

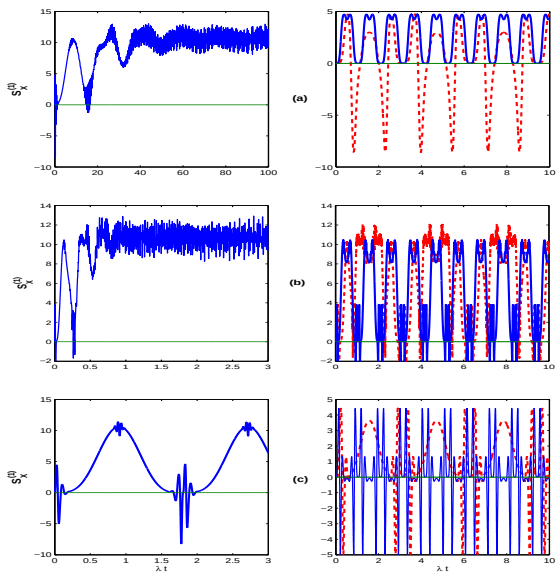

Fig. 8: The normal squeezing in terms of the scaled time λt, $\bar{n} = 20$, $\phi = \pi/2; \theta = \pi/3$, for chosen parameters similar to Fig.2.

For simplicity, we obtain the expectation value in the general form of the field operator $\widehat{a}^m$, for the model in the following form:

$$\begin{aligned} \langle \widehat{a}^m\rangle = |\alpha|^m \sum_n^\infty P_n \Big\{ \Big(& \psi_1(n+m,t)\psi_1^*(n,t) + \\ & \psi_2(n+m,t)\psi_2^*(n,t)\Big) \\ & + \sqrt{\frac{n(n-1)}{(n+m)(n+m-1)}}\psi_3(n+m-2,t)\psi_3^*(m-2,t) \\ & + \sqrt{\frac{n}{(n+m)}}\psi_4(n+r-1,t)\psi_4^*(n-1,t)\Big\}, \end{aligned} \tag{55}$$

where $\psi_{\mathcal{J}}^*$ denotes to the conjugate of $\psi_{\mathcal{J}}$. From the above equation the average values for the operators $\widehat{a}^\dagger$ and $\widehat{a}^{\dagger 2}$ can be obtained by putting $m = 1$ and $m = 2$, respectively. Also, it is well known that $\langle \widehat{a}^{\dagger m}\rangle$ is the conjugate of $\langle \widehat{a}^m\rangle$. Fig.8 shows the temporal behavior of the normal squeezing in .x-component fixed motion (left plots) and in x-component for motion case (right plots) in the nonlinear case $g(n) = 1$, $g(n) = n$ and $g(n) = \sqrt{n+\upsilon}$. Frames (a) and (b) have been plotted for one photon process, respectively. We can see from this figure that, the squeezing exists in the x_1 quadrature. Also, with comparing the left plots of Fig.8 one observes that, in addition to the fact that, in the single-photon process the system is always quadrature squeezed, the depth of squeezing is small. It should be noticed that, according to our further calculations, generally, there is squeezing in the quadratures x_1 and y_1 for the linear case $g(n) = 1$ and also for $g(n) = n$.

15 Summary and Conclusion

In this paper we studied the interaction between a four-level atom with a single-mode cavity field. Involving intensity dependent coupling, Fortunately, the wave function for the atomic system of λ -configuration is obtained when the atom is initially prepared in the excited state, the field is initially prepared in a coherent state. We investigated the atomic inversion, field entropy, Mandel Q parameter, mean photon number and normal squeezing as the most favorite nonclassicality features. Even though our formalism can be used for any nonlinearity function, we particularly have chosen the nonlinearity function $g(n)$ for our numerical calculations. The obtained results can be summarized as follows: The temporal evolution of field entropy, Mandel parameter, mean photon number and normal squeezing are sensitive to intensity-dependent coupling . The maximum value of the degree of entanglement measurement for the linear regime $(g(n) = 1)$ is greater than the nonlinear regime $(g(n) = n)$. Indeed, entering this nonlinearity function reduces the degree of entanglement measurement. The intensity-dependent coupling effected on the quantum statistical behavior of the atom-field state and changed to a full sub-Poissonian statistics for the single-photon process. Also, typical collapse-revival, as a nonclassical

behavior is seen. The time evolution of the mean photon number shows the collapse-revival phenomenon as a nonclassicality sign of the considered system. There is normal squeezing in the linear case and also nonlinear case in the presence of intensity-dependent coupling. The depth of the squeezing in the quadrature X_1 is smallers with the single-photon process. Finally, as well as different initial atom and radiation field states. Clearly our presented results are limited to the chosen $g(n)$ for the intensity dependent regime. Obviously, selecting other nonlinearity functions may lead to new and perhaps more interesting conclusions which can be done else where.

Acknowledgement

The authors are grateful to anonymous referee for a careful checking of the details and for helpful comments that improved this paper.

References

[1] E. T. Jaynes and F. W. Cummings: Proc. IEEE, **51**, 89 (1963).
[2] Z.D. Liu, S.-Y. Zhu and X.-S. Li: J. Mod. Optics **45**, 833 (1988).
[3] K. I. Osman and H. A. Ashi: Physica A **310**, 165 (2002).
[4] N. H. Abdel-Wahab: J. Phys. B: At. Mol. Opt. Phys. **41**, 105502 (2008).
[5] Y. Xue, G. Wang, J.-H. Wu. and J.-Y. Gao: Phys. Rev. A **75**, 063822 (2007).
[6] N. H. Abdel-Wahab: Mod. Phys. Lett. B **40**, 2801 (2008).
[7] X. Liu, Physica A **286**, 588 (2000).
[8] S. Abdel-Khalek and T. A. Nofal: Physica A **390**, 2626 (2011).
[9] H. Eleuch, S. Guerin and H.R. Jauslin: Phys. Rev. A **85**, 013830 (2012).
[10] D. Loss and D. P. Di Vincenzo: Phys. Rev. A **57**, 120 (1998).
[11] A. Abdel-Aty, L. Y. Cheong, N. Zakaria and N. Metwally, J. Comput. Theor. Nanosci. **12**, 2213 (2015).
[12] A. Abdel-Aty, M. Abdel-Aty, M. R. B. Wahiddin and A. Obada, Characteristics and distinctive features of entanglement in superconducting charge gubits, (Nova Science Publishers, Inc, USA, 2012), pp. 199-246.
[13] T. M. El-Shahat, S. Abdel-Khalek, M. Abdel-Aty and A. S-F. Obada: J. of Mod. Opt. **50**, 2013 (2003).
[14] C. H. Bennett: Phys. Today **48** 24 (1995); C. H. Bennett and D. P. Divincenzo: Nature 377, 389 (1995).
[15] J. I. Cirac and P. Zoller: Nature **404**, 579 (2000);
[16] D. P. Divincenzo: Science **270**, 255 (1995);
[17] L. K. Grover: Phys. Rev. Lett. **79**, 325 (1997);
[18] Z-Q. Yin, H-W. Li, W. Chen, Z-F. Han, and G-C. Guo: Phys. Rev. A **82** 042335(2010).
[19] T. G. Noh: Phys. Rev. Lett. **103**, 230501 (2009).
[20] W. H. Louisell, A. Yariv, and A. E. Siegman: Phys. Rev. **124**, 1646 (1961).
[21] C. H. Bennett and D. P. Di Vincenzo: Nature, **404**, 247 (2000).
[22] A.-H. M. Ahmed, L. Y. Cheong, N. Zakaria, N. Metwally and H. Eleuch, AIP Conference Proceedings **1482**, 373-375 (2012).
[23] M. S. Abdalla, M. M. Nassar: Ann. Phys. **324**, 637 (2009).
[24] W. H. Louisell: Coupled Mode and Parametric Electronics, Wiley, New York (1960).
[25] S. J. D. Phoenix and P. L. Knight: Phys. Rev. Lett. **66**, 2833 (1991)
[26] S. J. D. Phoenix and P. L. Knight: Ann. Phys., N. Y, **186**, 381 (1988)
[27] S. J. D. Phoenix and P. L. Knight: Phys. Rev. A **44**, 6023 (1991)
[28] T. M. El-Shahat: Appl. Math. Inf. Sci. **11**, No.5, 1479 (2017).
[29] M. sargent III, M. O. Scully, W.E. Lamb Jr.: Laser Physics, Addison-Wesley, Reading, MA, 1974.
[30] K. Zaheer and M. S. Zubairy: Phys. Rev. A **39**, 2000 (1989)
[31] Q.-C. Zhou and S.N. Zhu: Opt. Commun. **248**, 437 (2005)
[32] M. Abdel-Aty: Laser Phys. **16**, 1381 (2006), R. Roknizadeh and M. K. Tavassoly: J. Phys. A: Math. Gen. 37 8111 (2004), R. Roknizadeh and M. K. Tavassoly: J. Math. Phys. **46** 042110 (2005)
[33] A. A. Eied, S. A. Hanoura, and A.-S. F. Obada: Int. J. Theor. Phys. **51**, 2665 (2012)
[34] S. Singh, C.H. Raymond Ooi, and Amrita: Phys. Rev. A **86**, 023810 (2012)
[35] L. Mandel: Sub-Poissonian photon statistics in resonance fluorescence, Opt. Lett. **4** 205 (1979)
[36] H. I. Yoo and J. H. Eberly: Phys. Rev. A **118**, 239 (1985)
[37] H. Araki and E. LieB: Commun. math. Phys. **18**, 160 (1970)
[38] G. Benenti, G. Casati, G. Strini: Principles of Quantum Computation and Information; World Scientific: Singapore; Vol. **2**. (2007)
[39] V. Vedral and M. B. plenio: Phys. Rev. A **57**, 1619 (1998).
[40] D. Mchugh, M. Ziman and V. Buzk: Phys. Rev. A **74**, 4665 (2006).
[41] A. V. Peres: Phys. Rev. A **30**, 1610 (1984)
[42] R. Schack and C. M. Caves: Phys. Rev. E;**53**, 3257 (1996)
[43] Y.-b. Zhan: Phys. Lett. A **160** 498 (1991)

Tarek M. Elshahat is Associate Professor in the department of Mathematic, Al-Azhar Univrsity. He received the PhD degree in applied Mathematics "Quantum Opitcs" from the Faculty of Science, Al-Azhar University. He was visiting professor in the group of professor R. Tanas at Adam Mickiewicz University, Poznan, Poland. His research interests are in the areas of applied mathematics, quantum optics, quantum information.

Lamia E. Thabet is graduated from Mathematics and Physics Department, Taiz University, Yemen in 2002. She has completed her Master Science Courses with high grads in 2010 and MSC degree from Mathematics Department, King Saud University, Saudia Arabia. She was visiting scientist with the group of professor M.S. Abdalla, professor of Applied Mathematics at King Saud University. She will finish her PhD thesis soon at Mathematics department, Assiut University, Egypt. At present she is working as a Lecturer in Faculty of Science, Mathematics Department at Taiz University, Yemen. At present her research interests are the problems of the interaction between spins, quantum optics and quantum information.